

Article

Not peer-reviewed version

The Earth's Rotation-Related Seismicity as a Precursor to the 2023 Mw 7.8 Gaziantep, Turkey Earthquake

Yane Li , Xuezhong Chen ^{*} , Lijuan Chen

Posted Date: 3 August 2023

doi: 10.20944/preprints202308.0209.v1

Keywords: Earth's rotation-related; seismicity; the Mw 7.8 Turkey earthquake; Schuster test; precursor



Preprints.org is a free multidiscipline platform providing preprint service that is dedicated to making early versions of research outputs permanently available and citable. Preprints posted at Preprints.org appear in Web of Science, Crossref, Google Scholar, Scilit, Europe PMC.

Copyright: This is an open access article distributed under the Creative Commons Attribution License which permits unrestricted use, distribution, and reproduction in any medium, provided the original work is properly cited.

Article

The Earth's Rotation-Related Seismicity as a Precursor to the 2023 M_w 7.8 Gaziantep, Turkey Earthquake

Yane Li ^{1*}, Xuezhong Chen ^{1,*} and Lijuan Chen ²

¹ Institute of Geophysics, China Earthquake Administration, Beijing, China; liyane05@cea-igp.ac.cn(Y.L.), chenxz@cea-igp.ac.cn(X.C.)

² Chongqing Earthquake Administration, Chongqing, China; chenlijuan@cea-igp.ac.cn

* Correspondence: liyane05@cea-igp.ac.cn, chenxz@cea-igp.ac.cn

Abstract: For earthquakes ($M \geq 4.0$) occurring along and around the East Anatolian fault zone and the Dead Sea fault zone between January 2002 and December 2022, we analyzed the correlation between the Earth's rotation and the earthquake occurrence before the M_w 7.8 Gaziantep, Turkey earthquake occurring on 6 February 2023. We statistically evaluate the Earth's rotationally dependent seismicity. The results were judged by the P -value. There was a clear downward trend in the P -values from early 2020 to late 2022 in the study region. Starting in early 2021, the P -value drops below 0.1%, corresponding significant correlation between the Earth's rotation and the earthquake occurrence. We also calculated the spatial distribution of the P -values and obtained a result showing a low P -value area in the vicinity of the northeastern end of the aftershock zone. Although the stress caused by the Earth's rotation is very weak, when the focal medium is loaded to the critical state to release a large earthquake, the stress due to the Earth's rotation could control the earthquake occurrence. Therefore, the lower P -values obtained in this study indicates the Earth's rotation-related seismicity prior to the M_w 7.8 Turkey earthquake and could be considered as its precursor.

Keywords: Earth's rotation-related; seismicity; the M_w 7.8 Turkey earthquake; Schuster test; precursor

1. Introduction

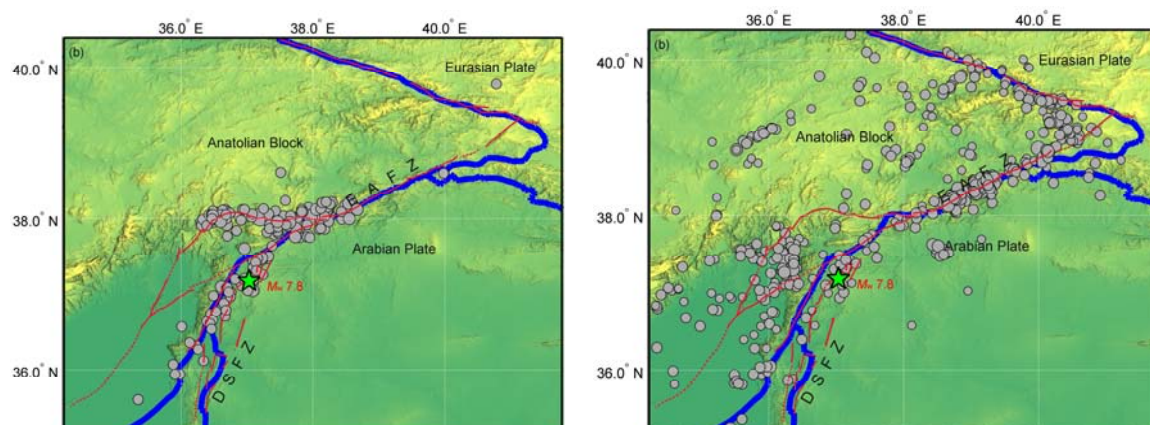
The physical essence of earthquakes is instability or failure of a stressed medium under the action of tectonic stress. When an earthquake occurs, the accumulated stress is quickly released. Based on rock test results, a focal fault will experience two stages before its failure: a stress-increase stage and a sub-instability stage[1,2]. During the latter the focal medium becomes extremely unstable and is approaching instability, where the time of earthquake occurrence can be controlled by weak stress perturbations that make some earthquakes occur more easily than usual. Although the stress changes ($\sim 1\text{Pa}$) due to the variation in the rate of Earth's rotation in the crust are quite tiny[3], when a strong earthquake is approaching, earthquakes in and around the focal medium would be susceptible to the weak changes of stress, resulting in a strong correlation between the Earth's rotation and the earthquake occurrence. Significant correlations were found between the Earth's rotation and the occurrence of earthquakes occurring before some strong earthquakes[4–9]. On 6 February 2023 an M_w 7.8 earthquake occurred in Gaziantep, Turkey with its epicenter located at 37.1662°N , 37.0421°E by the USGS Network. In the present study, we focused on this event to investigate the correlation between the Earth's rotation and the occurrence of earthquakes that occurred in and around its source region during pre-quake time interval.

2. Data and Methods

The 2023 Gaziantep M_w 7.8 earthquake occurred at the junction of the East Anatolian fault zone (EAFZ) with the Dead Sea fault zone (DSFZ). Its focal mechanism solutions indicate a steeply dipping fault plane striking NE-SW with a left lateral slip, or one striking NW-SE with right lateral slip. Aftershocks of the Gaziantep earthquake spread along the direction of NE-SW (Figure 1a). According to this, the Gaziantep earthquake ruptured on a left-slip plane striking NE-SW due to the relative motion between the Arabian plate and the Anatolian block.

Earthquakes used in this study were obtained from the USGS earthquake catalog (<https://earthquake.usgs.gov/earthquakes/search/>). The epicenter distribution of aftershocks of the M_w 7.8 Gaziantep earthquake were showed in Figure 1a (grey circles). The epicenters of earthquakes of $M \geq 3.0$ that occurred from January 2002 to December 2022 were plotted in Figure 1b. The spatial distribution of seismic numbers was obtained from the earthquakes in Figure 1b applying a spatial window of $1.0^\circ \times 1.0^\circ$ moved by 0.1° in both the latitudinal and longitudinal directions (Figure 1c). Three higher seismic frequency areas are located near the M_w 7.8 Gaziantep mainshock, at the central segment and near the junction of the EAFZ and the North Anatolian fault zone (EAFZ), respectively. For analysis of the P -value as a function of time, we considered an area of $\sim 400\text{km} \times 230\text{ km}$ as the study region (Figure 1c, the green boxed region) that covers the aftershock zone of the M_w 7.8 Gaziantep mainshock and two nearby higher seismic frequency areas. For all earthquakes in Figure 1b, we considered the completeness of earthquake catalogue with respect to the observed Gutenberg-Richter relationship via visual inspection. The event frequency-magnitude plot (Figure 2) suggests the threshold of completeness to be $M_c = 4.0$. For calculation of the P -value as a function of time we took 190 earthquakes of $M \geq 4.0$ that occurred in the study region from January 2002 to December 2022. For mapping the spatial distribution of the P -values, all earthquakes ($M \geq 4.0$) in Figure 1b were used.

The data of length of day relating to the Earth's rotation was acquired from the Earth Orientation Center (<http://hpiers.obspm.fr/eop-pc>). The raw data of length of day with the standard length of day (24 hours) subtracted is shown in Figure 3a. The variation of the length of day consists of different periodic components, which mainly include the long period component with a period of more than ten years, the seasonal component with a period of more than one month and less than one year, and the short period component with a period of less than one month. The nine-day-cycle component is contained in the short period component and is caused by atmospheric effects[10]. We will use the nine-day-cycle component to investigate the correlation between the Earth's rotation and the occurrence of earthquakes occurring prior to the 2023 M_w 7.8 Gaziantep event in this article. The nine-day-cycle component of the length of day is plotted in Figure 3b, obtained by band-pass filtering with a period band between 8d and 10d.



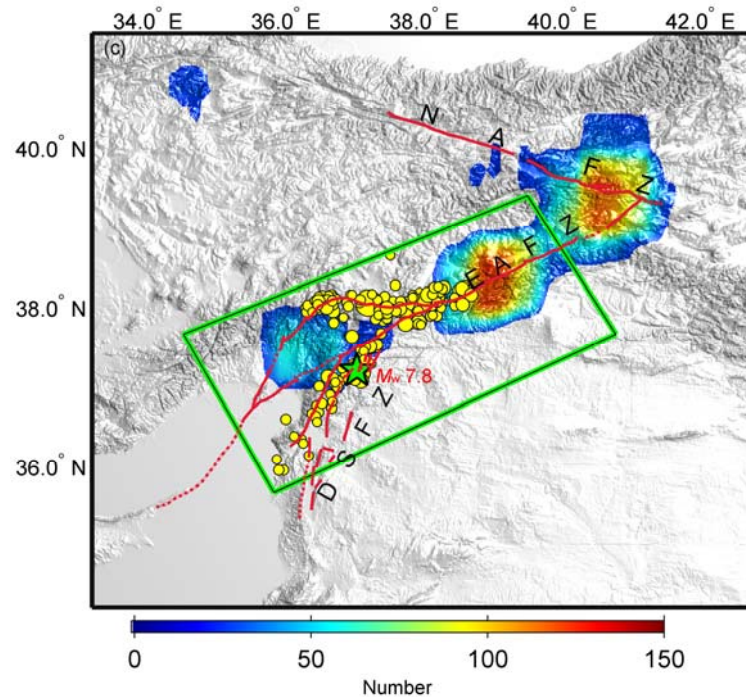


Figure 1. (a) The epicenter distribution of aftershocks of the M_w 7.8 Gaziantep earthquake occurring at the junction of the East Anatolian fault zone (EAFZ) with the Dead Sea fault zone (DSFZ). Grey circles show the epicenters of the aftershocks of $M \geq 4.0$ that occurred from 6 to 8 February, 2023. (b) Epicenters of earthquakes ($M \geq 3.0$) that occurred from 2002 to 2022. (c) Map showing the spatial distribution of seismic frequency obtained from earthquakes plotted in Figure 1b. Yellow circles are epicenters of aftershock events. In each picture, the green star represents the epicenter of the M_w 7.8 mainshock, the thick blue lines mark the boundaries between the different plates, the thin red lines show the active fault traces and the red boxed region shows the study area.

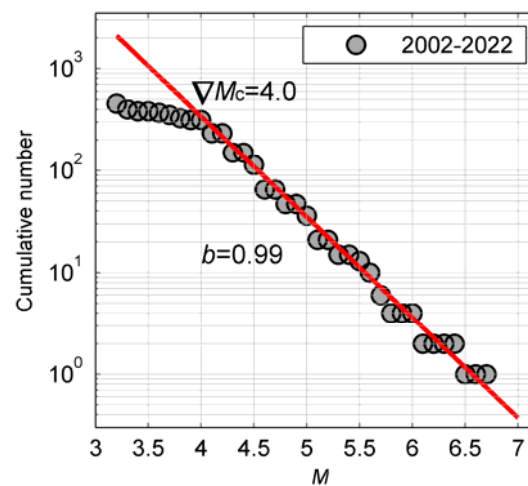


Figure 2. Cumulative number of earthquakes versus magnitude.

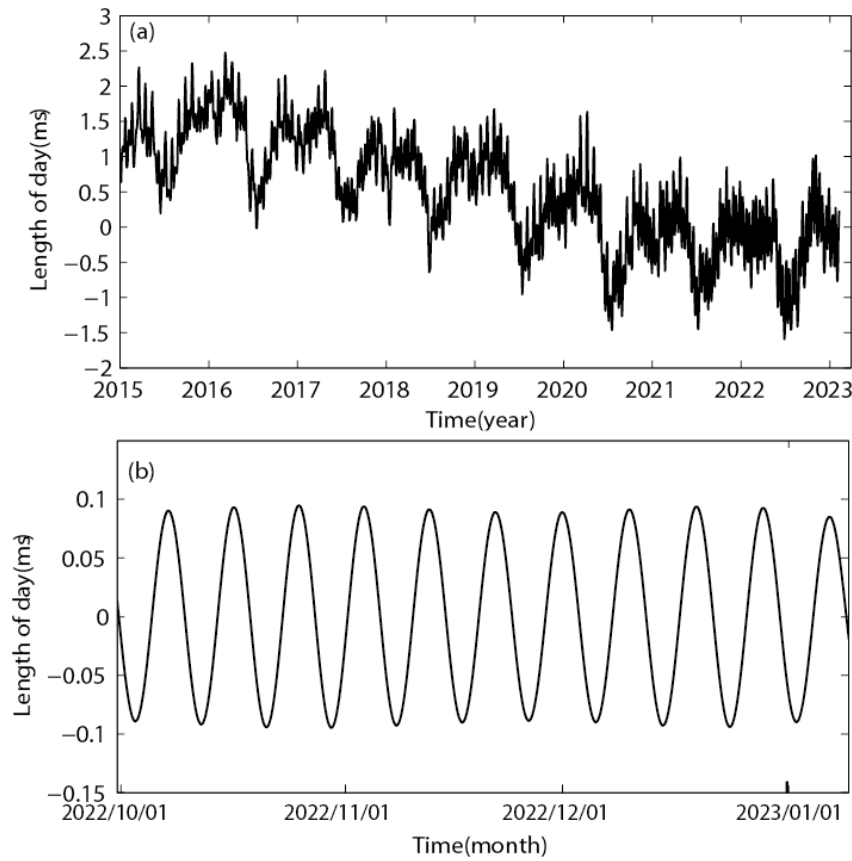


Figure 3. The length of day relating to the Earth's rotation versus time. (a) The raw data. (b) The nine-day-cycle variations in the length of day (filtered with a period band between 8d and 10d).

We statistically examined the correlation between the Earth's rotation and the earthquake occurrence. The used method has been applied to investigate tidal triggering of earthquakes[11–13]. Based on a temporal change series of length of day, the phase angle of the Earth's rotation at the occurring time of each earthquake can be calculated. The phase angle is defined as 0° at each maximum of the rate of the Earth's rotation, -180° at the first minimum on the left of the maximum, and 180° at the first minimum on the right one. The phase angle at the occurring time of an earthquake is calculated according to the following formula.

$$\left. \begin{aligned} \theta &= 180^\circ \times \frac{t_e - t_0}{t_0 - t_{-180}}, & t_e < t_0 \\ &= 180^\circ \times \frac{t_e - t_0}{t_{180} - t_0}, & t_e \geq t_0 \end{aligned} \right\} \quad (1)$$

Where t_e is the occurring time of an earthquake, t_0 the time at the maximum of length of day immediately before or after t_e , t_{-180} and t_{180} are the times at the minimum of length of day immediately before and after t_e respectively. With the phase angles of all earthquakes, we can statistically judge whether there is a significant correlation between those earthquakes and Earth's rotation by use of Schuster's test. The results were valued by P -value between 0 and 1. The P -value of N earthquakes can be obtained on the base of the following formulas.

$$P = e^{-\frac{R^2}{N}} \quad \left. \begin{aligned} R = \sqrt{\left(\sum_{i=1}^N \sin \theta_i\right)^2 + \left(\sum_{i=1}^N \cos \theta_i\right)^2} \end{aligned} \right\} \quad (2)$$

Where, θ is the phase angle of the i -th earthquake, $N > 10$. In general, if $P \leq 5\%$, the earthquakes could be non-random[14,15].

3. Results

For 190 earthquakes of $M \geq 4.0$ that occurred in the study region from January 2002 to December 2022, we examined the correlation between the nine-day-cycle variation of the Earth's rotation and the earthquake occurrence. The result is evaluated by the P -value. First, we determined the phase angle of the Earth's rotation at the occurring time of each earthquake on the base of equation (1) from the temporal change series of length of day (Figure 3b), then P -values as a function of time can be obtained via considering an eight-year time window moving 6 months at a time (Figure 4a). We calculated the P -value of each window according to equation (2), and took the occurring time of the last earthquake in each window as the time of P -value. The minimum number of earthquakes in all time windows is 46, the maximum 102 and the mean 63. Therefore, the requirement of earthquake number greater than 10 for the analysis can be met. A total of 40 P -values were calculated, of which only 8 are below 5%. This can be found in Figure 4a, where the P values were between 7% and 98% until April 2020 and no significant correlation can be found during this period. The P value dropped to $\sim 0.8\%$ in the beginning of August 2020, approached the lowest value (0.001%) in August 2022. The P values were below 0.1% from the beginning of 2021 to December 2022, therefore, a higher correlation between the earthquake occurrence and the Earth's rotation occurred in this period due to the focal medium's approaching instability.

The distribution of phase angles was obtained for ninety-seven earthquakes occurring when the P -value is at its lowest (Figure 4b), the corresponding time period is from September 2014 to August 2022. We found that most of these earthquakes occurred more easily when the phase angle was between -70° and 30° , this phase angle range corresponds to the increasing stage of the linear acceleration of Earth's rotation[9]. Thus, it is the increasing acceleration of Earth's rotation that controls the occurrence of earthquakes preceding the $M_w 7.8$ Gaziantep, Turkey earthquake.

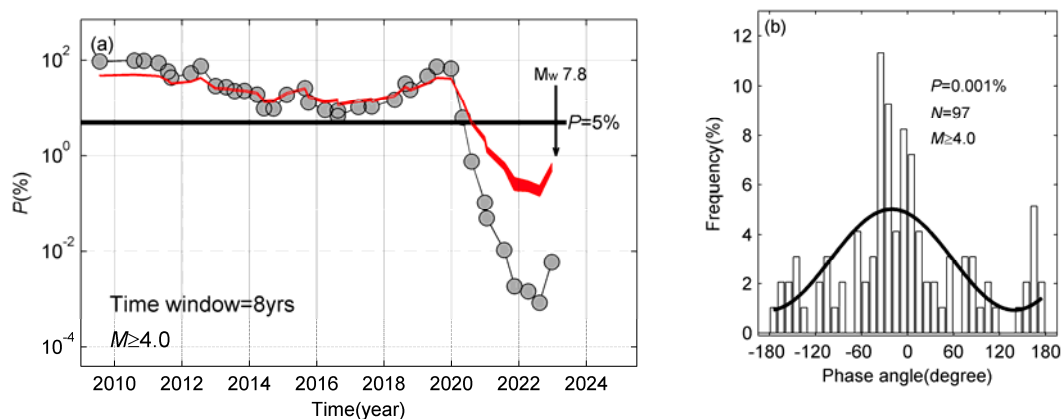


Figure 4. (a) P -value as a function of time in the study region. the downward arrow " shows the occurrence time of the $M_w 7.8$ Gaziantep event, the red area shows the 95% confidence limit of the P -value obtained by the bootstrap method. (b) Histogram showing the frequency of the phase angle of earthquakes occurring from September 2014 to August 2022. The thick solid curve denotes sinusoidal function fitted to the frequency distribution.

The bootstrap method is widely used for analyzing the statistical uncertainty [16,17]. It is based on the simulation of large number of data sets directly from the real experimental set of the events. The statistical fluctuations of the parameters are estimated using the simulated data sets for the investigated phenomenon. The simulation is based on the return-back sampling. That is, each simulated data set is randomly selected from the experimental data set without taking into account whether some events already have been taken to create this particular new data set or not. Any event from the initial set of the experimental data can be taken once, more than once, or cannot be taken at all. Each simulated data set contains the same number of events as the original experimental one. When the simulation of a large number of the new data sets is finished then relevant parameters are calculated for each of them. After this, it is easy to get the means and 95% confidence ranges of these parameters. We analyzed the confidence intervals of P values for each bin in Figure 4a based on bootstrap method. A sample of size 3000 is taken in the analysis. The confidence intervals of 95% of P values for each bin are shown by the red area in Figure 4a. In December 2021, the P value dropped to a value between 0.25% and 0.44%, far below 5%.

The spatial distribution of the P -values for earthquakes ($M \geq 4.0$) occurring from September 2014 to August 2022 is shown in Figure 5a. A time interval of ten years was used for obtaining the spatial distribution of the P -values. A rectangle region with latitude range from 34°N - 40.5°N and longitude range from 33°E - 42°E was considered. A circular spatial window of a radius of 100km moving by 0.1° in along-latitude and along-longitude directions was used. When earthquakes in a window are over 10, P -value can be worked out. The spatial distribution of $P < 1\%$ was plotted in Figure 5b, where it can be found that low P -values located in the northeast of the study area for analysis of the P -value as a function of time. Two mainshocks occurred on 6 February 2023, their magnitudes are $M_w 7.8$ and $M_w 7.5$ respectively. Their locations are shown by stars in Figure 5b. The minimum distances between their epicenters and the edge of the area with P -values less than 1% less are 138km and 83km respectively.

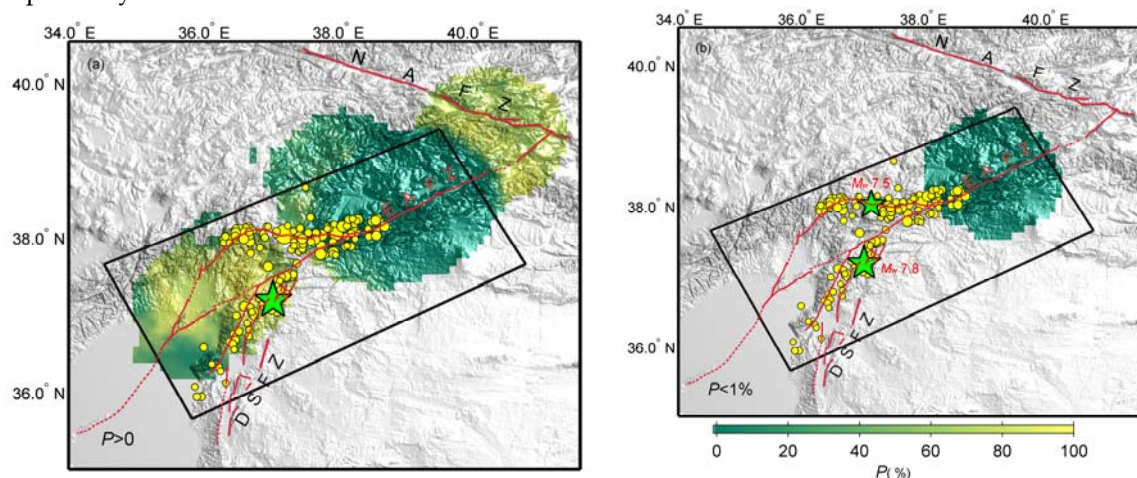


Figure 5. Spatial distribution of the P -values obtained using earthquakes occurring from September 2014 to August 2022. A circular spatial window of a radius of 100km moving by 0.1° in both along-latitude and along-longitude directions was used. The star shows the epicenters of the $M_w 7.8$ and 7.5 mainshocks. (a) $P > 0$. (b) $P < 1\%$. Yellow circles are epicenters of aftershock events.

4. Discussion

We investigated the correlation between the Earth's rotation and earthquakes that occurred before the $M_w 7.8$ Gaziantep earthquake. For earthquakes of $M \geq 4.0$ in the study area we calculated the P -value as a function of time. We discovered lower P -values only occurred about two years prior to the $M_w 7.8$ Gaziantep earthquake. Earthquakes happened more frequently when the phase angle was between -70° and 30° , corresponding to the increasing period of the linear acceleration of the Earth's rotation.

Furthermore, we calculated the spatial distribution of the P -values using earthquakes ($M \geq 4.0$) occurring from September 2014 to August 2022 and found that low P -values ($P < 1\%$) covered an area less than 140km northeast of the epicenter of the M_w 7.8 Gaziantep earthquake.

We also investigated the correlation between the rotation of the Earth and the occurrence of earthquakes using the seasonal component and did not find any significant correlation. This may be related to the critical stiffness of the focal medium. It was found based on slider-block models of slip that slip can amplify dramatically under the action of given stress within a narrow band of resonant periods [18]. Slip response amplifies significantly for a narrow range of periods near the critical period T_c when stiffness k is equal to the critical stiffness k_c , and at shorter periods when k is greater than k_c [19].

It has been well-known that when a stressed medium is approaching failure, it will reach a critical state. Under this condition, when the period of the Earth's rotation is within a narrow band of resonant periods, seismicity could be significantly correlated to the Earth's rotation.

5. Conclusions

From the above results, the significant Earth's rotation-related seismic activity indicated that the focal medium in the region around the M_w 7.8 Gaziantep earthquake was at a critical state. In other words, the focal medium has become extremely unstable, and could failure at any moment to release a strong earthquake. Therefore, we suggest that the Earth's rotation-related seismicity prior to the M_w 7.8 Gaziantep, Turkey earthquake could be considered as one of its precursors.

Author Contributions: X.C. contributed to the conceptualization; supervised the research; formulated the research questions; and specified the manuscript contents, discussed with Y.L. and J.C., and prepared the manuscript. Y.L. participated in the collection of references, performed the collation of the earthquake catalog used and plotting diagrams, submitted the manuscript, and provided constructive suggestions to the study. L.C. participated in the collection of references and provided constructive suggestions to the study. All authors have read and agreed to the published version of the manuscript.

Funding: This research received no external funding.

Data Availability Statement: Not applicable.

Acknowledgments: The authors express sincerely thanks to the journal editors for their help and beneficial comments to the manuscript.

Conflicts of Interest: The authors declare no conflict of interest.

References

1. Ma, J.; Guo, Y. Accelerated synergism prior to fault instability: evidence from laboratory experiments and an earthquake case (in Chinese with English abstract). *Seismol. Geol.* 2014, 36, 547–561.
2. Ma, J. On “whether earthquake precursors help for prediction do exist?” (in Chinese with English abstract). *Chinese Sci. Bull.* 2016, 61, 409–414.
3. Chen, X.; Wang, H.; Wang, S.; Wei, Y.; Guo, X.; Chen, L.; Li, Y. Effect of the Earth's rotation deceleration on the occurrence of the 2008 Wenchuan M_s 8.0 earthquake (in Chinese with English abstract). *Earthquake* 2018, 38, 127–136.
4. Wei, Y.; Chen, X.; Li, Y. Relation between Earth's rotation and small earthquakes occurring before the M_s 7.8 Tangshan mainshock (in Chinese with English abstract). *Chinese Sci. Bull.* 6, 1822–1828.
5. Chen, X.; Li, Y. Relationship Between the deceleration of Earth's rotation and earthquakes that occurred before the M_s 8.0 Wenchuan earthquake. *Pure and Applied Geophysics* 176, 5253–5260.
6. Chen, X.; Li, Y.; Wei, Y. Earth's rotation-triggered earthquakes before the 2018 M_s 5.7 Xingwen earthquake. *Earthquake Science* 32, 35–39.
7. Chen, X.; Li, Y.; Wei, Y.; Guo, X.; Chen, L. Relationship between the Earth's rotation rate and earthquakes occurring prior to the 2011 M_w 9.1 Tohoku-Oki Japan earthquake (in Chinese with English abstract). *Chinese Journal of Geophysics* 2020, 63, 440–444.
8. Chen, X.; Li, Y.; Chen, L. Why the M_w 6 Parkfield earthquake expected in the 1985–1993 interval was postponed till 2004?. *Geomatics, Natural Hazards and Risk* 2022, 13, 2151–2165.
9. Li, Y.; Chen, X.; Chen, L. The Earth's rotation-triggered earthquakes preceding the occurrence of the 2019 M_w 7.1 Ridgecrest earthquake. *Geomatics, Natural Hazards and Risk* 2022, 12, 3021–3034.

10. Han, Y.; Li, Z. Analysis of main middle and short periods in the variation of the Earth's rotation(in Chinese with English abstract). *Chinese Journal of Geophysics* 2002, 17, 349-352.
11. Tanaka, S.; Ohtake, M.; Sato, H. Spatio-temporal variation of the tidal triggering effect on earthquake occurrence associated with the 1982 South Tonga earthquake of M_w 7.5. *Geophys. Res. Lett.* 2002, 29, 3-1-3-4.
12. Tanaka, S. Tidal triggering of earthquakes precursory to the recent Sumatra megathrust earthquakes of 26 December 2004 (M_w 9.0), 28 March 2005 (M_w 8.6), and 12 September 2007 (M_w 8.5). *Geophys. Res. Lett.* 2010, 37;L02301.
13. Tanaka, S. Tidal triggering of earthquakes prior to the 2011 Tohoku-Oki earthquake (M_w 9.1). *Geophys. Res. Lett.* 2012, 39, L00G26.
14. Tsuruoka, H.; Ohtake, M.; Sato, H. Statistical test of the tidal triggering of earthquakes: Contribution of the ocean tide loading effect. *Geophysical Journal International* 122,1995, 183-194.
15. Heaton, T. H. Tidal triggering of earthquakes. *Geophys. J. R. Astr. Soc.* 1975, 43, 307-326.
16. Efron, B. Bootstrap methods: Another look at the jackknife. *Annals of Statistics* 1979,7, 1-26.
17. Matsuyama, T. An application of bootstrap method for analysis of particle size distribution. *Advanced Powder Technology* 2018,29, 1404-1408.
18. Perfettini, H.; Schmittbuhl, J.; Rice, J. R.; Cocco, M. Frictional response induced by time-dependent fluctuations of the normal loading. *J. Geophys. Res.* 2001, 106, 13455-13472.
19. Lowry, A. R. Resonant slow fault slip in subduction zones forced by climatic load stress. *Nature* 2006, 442, 802-805.

Disclaimer/Publisher's Note: The statements, opinions and data contained in all publications are solely those of the individual author(s) and contributor(s) and not of MDPI and/or the editor(s). MDPI and/or the editor(s) disclaim responsibility for any injury to people or property resulting from any ideas, methods, instructions or products referred to in the content.